www.nature.com/cr
www.cell-research.com

Cell Research

LETTER TO THE EDITOR

Structure of the mitochondrial TIM22 complex from yeast

Cell Research (2021) 31:366–368; https://doi.org/10.1038/s41422-020-00399-0

Dear Editor,

Mitochondria have more than 1000 proteins, most of which are encoded by nuclear DNA and imported from the cytosol.[1] A large group of multi-spanning membrane proteins, the solute carrier proteins, are imported from the cytosol by the translocase of the outer membrane (TOM) and translocated into the inner membrane (IM) by the TIM22 complex.[2] The TIM22 complex in *Saccharomyces cerevisiae* (*S. cerevisiae*) has seven subunits: Tim22, Tim18, Tim54, Sdh3, Tim9, Tim10, and Tim12. Tim22 is the core translocase subunit. The three small Tim proteins, Tim9, Tim10, and Tim12, are homologous to each other. Tim9 and Tim10 form hexameric chaperones in the intermembrane space (IMS) to deliver the polypeptide substrates from the TOM to the TIM22.[3] Tim9 and Tim10 become part of the TIM22 complex with the help of Tim12.[4] Tim54 likely interacts with Tim9-Tim10-Tim12 in the complex.[5] Sdh3 is a membrane component of respiratory complex II (succinate dehydrogenase, SDH). Tim18 is homologous to Sdh4, the partner of Sdh3 in respiratory complex II. The functions of Sdh3 and Tim18 in the TIM22 complex are less clear. Previous studies have suggested that driven by the membrane potential, the TIM22 complex might function as a twin-pore translocase.[6] However, it is poorly understood how the subunits of TIM22 assemble and accomplish protein translocation due to lack of high-resolution structural information. To address some of the fundamental questions in the field, we determined the electron cryo-microscopy (cryo-EM) structure of the endogenous TIM22 complex from *S. cerevisiae*.

To facilitate purification of the endogenous TIM22 complex, Tim18 in the yeast genome was fused with a C-terminal twin-strep tag. The structure of the purified TIM22 complex was determined at a resolution of 3.8 Å (Supplementary information, Figs. S1–S3). All the subunits could be identified in the structure.

The small Tim subunits in TIM22 form a hexameric ring and sit on the membrane with a ~45° tilt (Fig. 1a, b). The ring is similar to the crystal structure of the Tim9-Tim10 complex,[3] except that one of the Tim10 subunits is replaced by Tim12[4] (Fig. 1b). Tim12 is homologous to Tim10 and has an additional C-terminal helix that intercalates between the N- and C-terminal helices of one Tim9 subunit (Supplementary information, Fig. S4). Interestingly, strong density blobs are also observed in the same cleft of the other two Tim9 subunits (Supplementary information, Fig. S4b, c). Although the exact sequences could not be identified, one of the density blobs is extended from Tim54 and the other one is likely from the N-terminal segment of Tim22. Therefore, the hydrophobic clefts of all three Tim9 subunits are occupied by the peptides, whereas the hydrophobic clefts of Tim10 and Tim12 are open for substrate binding.[7]

The core structure of Tim54 is well resolved in the density map, although the model is incomplete due to large disordered regions. Tim54 has a typical α/β motif in the IMS. A four-stranded β sheet is sandwiched by four α-helices, with α1 and α4 on one side, and α2 and α3 on the other side (Supplementary information, Fig. S5a). Similar α/β motifs are found in the lipid kinases, such as diacylglycerol kinases (DGK) and sphingosine kinases[8] (Supplementary information, Fig. S5b, c). Interestingly, the human TIM22 complex contains mitochondrial acylglycerol kinase (AGK), but not Tim54. Tim54 and AGK may have similar folds and functions in the TIM22 complex, although the two subunits have no sequence homology. Tim54 is anchored on the membrane by an N-terminal transmembrane segment (TM) (residues 37–71, α0) and an amphipathic helix from α4 (Supplementary information, Fig. S5a). Tim54 may help to hold the ring of the small Tim subunits in the 45°-tilted conformation as it is the only subunit that has interactions with the ring in the IMS (Fig. 1a).

Tim18, Sdh3, and Tim22 are close to each other in the membrane. Together, the three membrane subunits provide a docking platform for the small Tim subunits (Fig. 1a). Both Tim18 and Sdh3 have three TMs and an amphipathic helix on the IMS side (Fig. 1c). Tim18 and Sdh3 form a heterodimer with pseudo two-fold symmetry, similar to the organization of Sdh3-Sdh4 in mitochondrial respiratory complex II.[9] Tim22 has four TMs that form a curved surface, with the concave side opening to the lipids and the convex side facing Tim18 (Fig. 1c). Consistent with the biochemical data,[10] the conserved cysteine residues, 42 and 141, form a disulfide bond between TMs 1 and 2 (Fig. 1c).

The TIM22 complex has some unusual electrostatic features in the membrane (Fig. 1d). While the other subunits have the typical charge and hydrophobicity distributions of membrane proteins, the concave surface of Tim22 has a large negatively charged patch exposed to the membrane on the IMS side. The transmembrane distance is relatively short due to the TM2-TM3 split on the matrix side (Fig. 1e). Indeed, on the IMS side, Tim22 has a completely conserved glutamic acid (E140) of TM2 next to the disulfide bond, as well as a conserved aspartic acid (D190) in TM4[11] (Fig. 1e). The TM2-TM3 split is bordered by two lysine residues pointing to each other, a conserved lysine (K127) of TM2 and a lysine in the loop between TMs 3 and 4 (K169) (Fig. 1e). Mutagenesis studies show that the single mutations, E140A and K127A, greatly impaired yeast cell growth (Fig. 1f), while the assembly of the TIM22 complex in the mutants was not affected (Supplementary information, Fig. S6). The double mutants, E140A/D190A and K127A/K169A, and the quadruple mutant are essentially lethal to yeast growth (Fig. 1f). The results highlight the critical roles of the charged residues for the proper functioning of Tim22.The structure of the TIM22 complex does not reveal an obvious translocation channel for substrate import. It is rather surprising as previous studies have suggested that the TIM22 complex might act as a twin-pore translocase.[6] One possible scenario could be that the current structure may represent an idle state or an intermediate state. Driven by the membrane potential, the TIM22 complex, particularly the Tim22 subunit, may undergo conformational changes to oligomerize and form pores. Alternatively, the single Tim22 subunit may be sufficient to act as a TM insertase, similar to the bacterial insertase, YidC.[12] The completely conserved

Received: 29 April 2020 Accepted: 24 July 2020
Published online: 11 September 2020

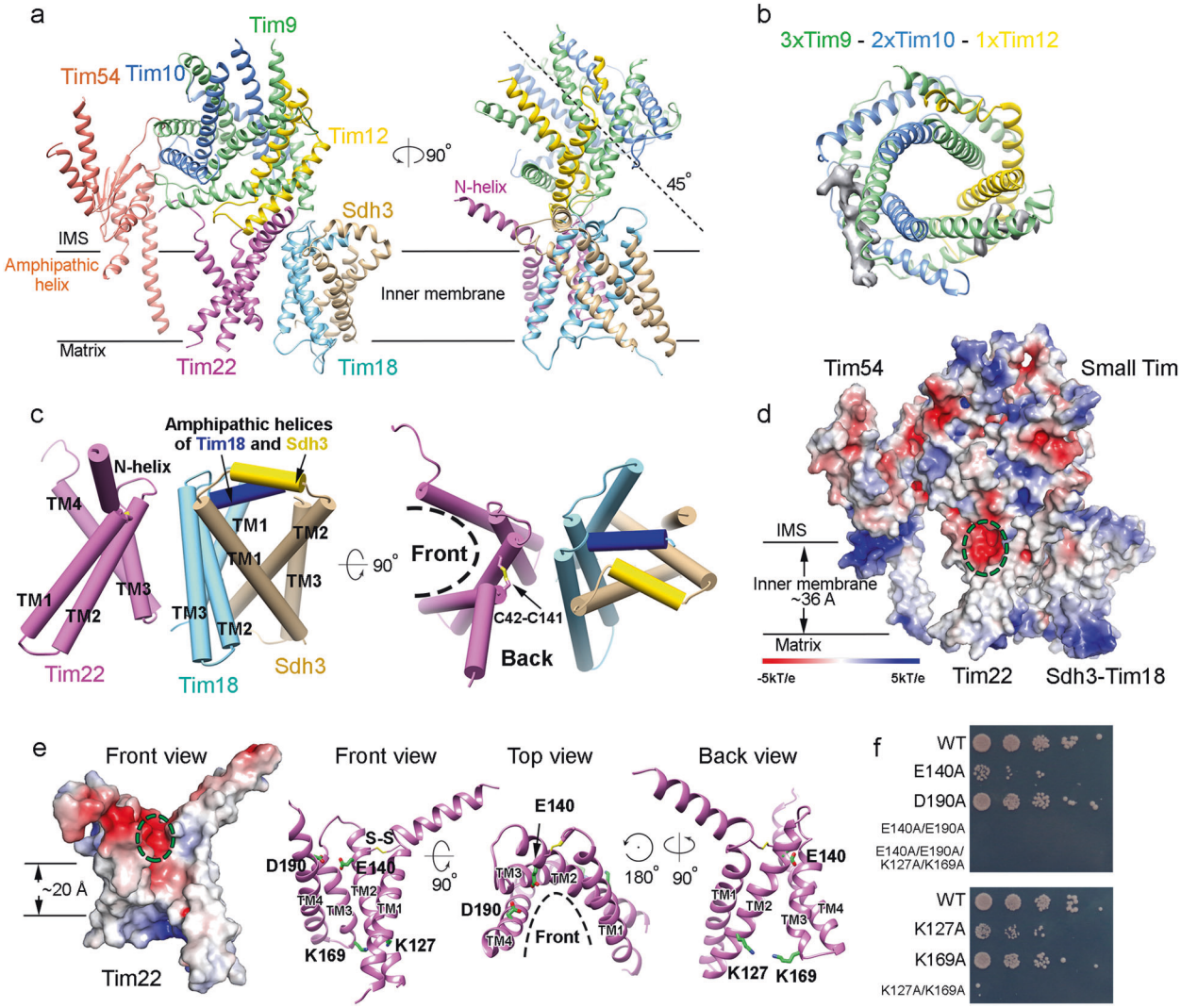

Fig. 1 Structure of the TIM22 complex. a Ribbon diagrams of the TIM22 complex. The subunits are labeled. Tim22, Tim18, Sdh3, Tim9, Tim10, Tim12, and Tim54 are colored purple, light blue, tan, light green, blue, yellow, and salmon, respectively. The structure is shown in two views with 90° rotation (left and right panels). The inner membrane, IMS, matrix, and amphipathic helix of Tim54, as well as the N terminal helix of Tim22, are marked. The central axis of the small Tim ring is drawn to show the 45° tilt (right panel). **b** Top view of the Tim9-Tim10-Tim12 hexameric ring, viewed along the central axis. **c** Structure of Tim22-Tim18-Sdh3. The proteins are shown as cylinders. The TMs, the N-terminal helix of Tim22, and the amphipathic helices are labeled. The amphipathic helix of Tim18 is blue and the amphipathic helix of Sdh3 is yellow. The disulfide bond (C42-C141) of Tim22 that connects TM1 and TM2 is shown as sticks. The dashed curve indicates the opening of Tim22 to the membrane. **d** Electrostatic potential surface of the TIM22 complex. The view is the same as in **a** (left panel). The green dashed circle highlights the negatively charged concave surface. The electrostatic potential surfaces are calculated by using APBS with the default setting in PyMOL. **e** Structure of Tim22 in different views. Left panel, electrostatic potential of the concave surface of Tim22. The estimated thickness of the membrane is marked. Right panels, different views of Tim22. Conserved residues E140, D190, K127, and K169 are shown as sticks. The disulfide bond between TM1 and TM2 is shown and labeled. The dashed line demonstrates the curved surface that opens to the lipids. **f** Growth of the yeast cells with mutations in Tim22. 5-fold serial dilutions of Tim22 wild-type and mutant cells were spotted on to synthetic complete medium (glucose) +FOA plates and cultivated at 30 °C for 3 days.

E140 and K127 are only 12 residues away in TM2, with a linear distance of ~20 Å, about half of the thickness of the regular membranes (Fig. 1e). The distribution of the charged residues in the TMs of Tim22 may decrease the thickness of the local lipid membrane. The charged environment in the thinner membrane could greatly reduce the energy barrier for TM insertion.

The Tim9-Tim10 complex chaperones the polypeptide substrates from the TOM complex to TIM22. Tim9-Tim10 may deliver the substrates by making direct contact with the Tim22 complex. Indeed, during 2D classification, a top view of the complex with two rings was occasionally observed (Supplementary information, Fig. S2b). The "two-ring" view was similar to the results from negative stain EM,[6] both of which had a diameter of ~16 Å. The additional ring might be the Tim9-Tim10 complex. The polypeptide substrates carried by the Tim9-Tim10 ring might be passed directly to the Tim9-Tim10-Tim12 ring and then to Tim22, whose concave surface is well aligned with a substrate-binding cleft of Tim9-Tim10-Tim12 (Supplementary information, Fig. S7).

In summary, the structure of the TIM22 complex reveals a sophisticated organization of the seven subunits. Tim18-Sdh3 and Tim22 provide a docking platform for anchoring Tim9-Tim10-Tim12. Tim9-Tim10-Tim12 is at the center of the assembly, likely to receive the polypeptide substrates from Tim9-Tim10 and pass them to Tim22. Tim54 helps to hold Tim9-Tim10-Tim12 in a tilted

conformation. Tim22 may create a hydrophilic environment either inside a channel or in the membrane to facilitate TM insertion.

ACKNOWLEDGEMENTS

We thank Dr. Ningning Li, Dr. Guopeng Wang, and Dr. Ye Xiang for assistance with EM data analysis, Dr. Ning Gao for critical reading of the manuscript, the National Center for Protein Sciences at Peking University in Beijing, China, for assistance with protein purification and mass spectrometry, the Core Facilities at School of Life Sciences Peking University for assistance with negative staining EM, and the Electron Microscopy Laboratory of Peking University and the cryo-EM platform of Peking University for help with data collection. Computation was supported by the High-performance Computing Platform of Peking University. Q.L. is supported by Beijing Outstanding Young Scientist Program (BJJWZYJH01201910001005).

AUTHOR CONTRIBUTIONS

Y.Z., X.O., D.S., and X.Z. prepared the samples. Y.Z., X.O., and X.Wu performed cryo-EM sample preparation and data collection. X.Wang performed yeast genetics, Y.Z. and L. L. determined the structures. L.L. and Q.L. supervised the project. All authored are involved in preparing the manuscript.

ADDITIONAL INFORMATION

Supplementary information accompanies this paper at https://doi.org/10.1038/s41422-020-00399-0.

Competing interests: The authors declare no competing interests.

Yutong Zhang[1,2,3], Xiaomin Ou[1,2], Xuezheng Wang[2,3,4], Dongjie Sun[1,2], Xueyin Zhou[1,2,3], Xiaofei Wu[1,2], Qing Li[2,4] and Long Li[1,2]

[1]State Key Laboratory of Membrane Biology, Peking University, Beijing, China; [2]Peking-Tsinghua Center for Life Sciences, School of Life Sciences, Peking University, Beijing, China; [3]Academy for Advanced Interdisciplinary Studies, Peking University, Beijing, China and [4]State Key Laboratory of Protein and Plant Gene Research, Peking University, Beijing, China

These authors contributed equally: Yutong Zhang, Xiaomin Ou

Correspondence: Long Li (long_li@pku.edu.cn)

REFERENCES

1. Sickmann, A. et al. *Proc. Natl. Acad. Sci. USA* **100**, 13207–13212 (2003).
2. Wiedemann, N. & Pfanner, N. *Annu. Rev. Biochem.* **86**, 685–714 (2017).
3. Baker, M. J. et al. *Mol. Biol. Cell* **20**, 769–779 (2009).
4. Gebert, N. et al. *EMBO Rep.* **9**, 548–554 (2008).
5. Wagner, K. et al. *Mol. Biol. Cell* **28**, 4251–4260 (2008).
6. Rehling, P. et al. *Science* **299**, 1747 (2003).
7. Weinhäupl, K. et al. *Cell* **175**, 1365–1379 (2018).
8. Ma, Q., Gabelli, S. B. & Raben, D. M. *Adv. Biol. Regul.* **71**, 104–110 (2019).
9. Sun, F. et al. *Cell* **121**, 1043–1057 (2005).
10. Wrobel, L., Sokol, A. M., Chojnacka, M. & Chacinska, A. *Sci. Rep.* **6**, 27484 (2016).
11. Žárský, V. & Doležal, P. *Biol. Direct* **11**, 54–54 (2016).
12. Hennon, S. W., Soman, R., Zhu, L. & Dalbey, R. E. *J. Biol. Chem.* **290**, 14866–14874 (2015).